Title
Influence of regional-scale anthropogenic emissions on CO2 distributions over the western North Pacific

Journal
Journal of Geophysical Research, 108(D20)

ISSN
0148-0227

Authors
Vay, SA
Woo, J-H
Anderson, BE
et al.

Publication Date
2003

DOI
10.1029/2002jd003094

Influence of regional-scale anthropogenic emissions on CO_2 distributions over the western North Pacific

S. A. Vay,[1] J.-H. Woo,[2] B. E. Anderson,[1] K. L. Thornhill,[3] D. R. Blake,[4] D. J. Westberg,[3] C. M. Kiley,[5] M. A. Avery,[1] G. W. Sachse,[1] D. G. Streets,[6] Y. Tsutsumi,[7] and S. R. Nolf[8]

Received 30 October 2002; revised 20 February 2003; accepted 24 April 2003; published 12 September 2003.

[1] We report here airborne measurements of atmospheric CO_2 over the western North Pacific during the March–April 2001 Transport and Chemical Evolution over the Pacific (TRACE-P) mission. The CO_2 spatial distributions were notably influenced by cyclogenesis-triggered transport of regionally polluted continental air masses. Examination of the CO_2 to C_2H_2/CO ratio indicated rapid outflow of combustion-related emissions in the free troposphere below 8 km. Although the highest CO_2 mixing ratios were measured within the Pacific Rim region, enhancements were also observed further east over the open ocean at locations far removed from surface sources. Near the Asian continent, discrete plumes encountered within the planetary boundary layer contained up to 393 ppmv of CO_2. Coincident enhancements in the mixing ratios of C_2Cl_4, C_2H_2, and C_2H_4 measured concurrently revealed combustion and industrial sources. To elucidate the source distributions of CO_2, an emissions database for Asia was examined in conjunction with the chemistry and 5-day backward trajectories that revealed the WNW/W sector of northeast Asia was a major contributor to these pollution events. Comparisons of NOAA/CMDL and JMA surface data with measurements obtained aloft showed a strong latitudinal gradient that peaked between 35° and 40°N. We estimated a net CO_2 flux from the Asian continent of approximately 13.93 Tg C day^{-1} for late winter/early spring with the majority of the export (79%) occurring in the lower free troposphere (2–8 km). The apportionment of the flux between anthropogenic and biospheric sources was estimated at 6.37 Tg C day^{-1} and 7.56 Tg C day^{-1}, respectively. *INDEX TERMS:* 0345 Atmospheric Composition and Structure: Pollution—urban and regional (0305); 0365 Atmospheric Composition and Structure: Troposphere—composition and chemistry; 0368 Atmospheric Composition and Structure: Troposphere—constituent transport and chemistry; *KEYWORDS:* carbon dioxide, Asian emissions, CO_2 flux

Citation: Vay, S. A., et al., Influence of regional-scale anthropogenic emissions on CO_2 distributions over the western North Pacific, *J. Geophys. Res.*, *108*(D20), 8801, doi:10.1029/2002JD003094, 2003.

1. Introduction

[2] The global burden of atmospheric CO_2 has increased by approximately 100 ppmv in the last 150 years due primarily to human activities associated with the combustion of fossil fuels. This is important with respect to geological time scales as it has risen to that level at a rate at least 10 times faster than at any other time in the past 420,000 years [*Falkowski et al.*, 2000]. Prior to the 1980s, the largest contributors to CO_2 emissions from this source were the industrialized countries of North America and Europe; however, Asian emissions have since surpassed those of any other continent [*Akimoto and Narita*, 1994; *Siddiqi*, 1996]. This change is attributable to substantial increases in energy use triggered by the rapid economic and population growth of many Asian countries. Over time, this growth has resulted in a slow southerly shift in the band of maximum CO_2 emissions from 50°–55°N to 35°–40°N [*Akimoto and Narita*, 1994; *Andres et al.*, 1999].

[3] Within the Pacific Rim region of Asia, China (1042 Tg C yr^{-1}) and Japan (328 Tg C yr^{-1}) have the highest reported CO_2 emissions from anthropogenic sources for the year 2000 [*Streets et al.*, 2003]. Through long-range transport processes air parcels augmented with these emissions can be propagated away from urban and industrial centers thus affecting the CO_2 spatial distributions over widespread geographical regions [*Merrill et al.*, 1989; *Kotamarthi and Carmichael*, 1990]. Airborne observations of atmospheric CO_2 in this region began in 1979 with

[1]NASA Langley Research Center, Hampton, Virginia, USA.
[2]Center for Global and Regional Environmental Research, University of Iowa, Iowa City, Iowa, USA.
[3]Science Applications International Corporation, Hampton, Virginia, USA.
[4]Department of Chemistry, University of California, Irvine, California, USA.
[5]Department of Meteorology, Florida State University, Tallahassee, Florida, USA.
[6]Decision and Information Sciences Division, Argonne National Laboratory, Argonne, Illinois, USA.
[7]Atmospheric Environment Division, Japan Meteorological Agency, Tokyo, Japan.
[8]Computer Sciences Corporation, Hampton, Virginia, USA.

0148-0227/03/2002JD003094

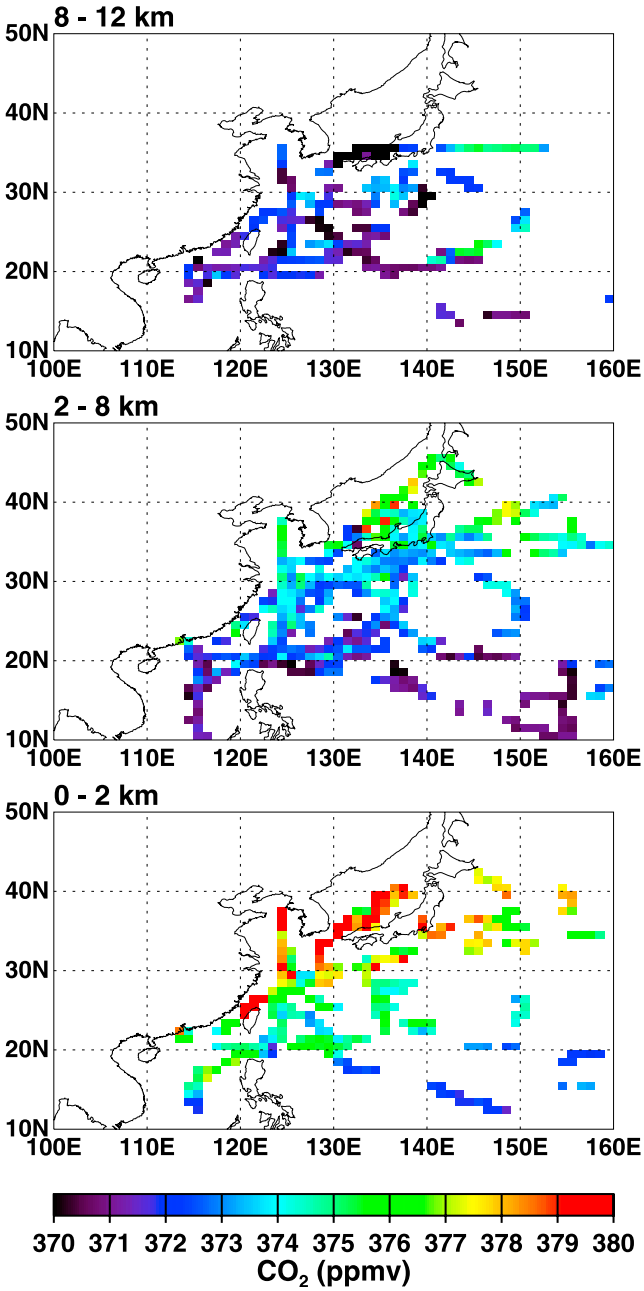

Figure 1. Regional distribution of CO_2 during TRACE-P for the altitude regime of 0–2 km, 2–8 km, 8–12 km. Data were grouped into 1° latitude by 1° longitude bins and then averaged.

tropospheric measurements over Japan and have continued in subsequent years primarily from commercial aircraft operating in the upper troposphere and lower stratosphere [*Tanaka et al.*, 1983, 1987, 1988; *Nakazawa et al.*, 1991, 1993; *Anderson et al.*, 1996; *Matsueda and Inoue*, 1996, 1999; *Matsueda et al.*, 2002]. These extensive measurements have provided valuable information on the three-dimensional (3-D) spatial distributions of CO_2 as well as the secular increase and seasonal variability particularly in response to the phase of the ENSO cycle.

[4] To investigate the magnitude of the human impact on atmospheric CO_2 and other trace species over the western North Pacific, the Transport and Chemical Evolution over the Pacific (TRACE-P) mission was conducted in March–April, 2001. Reported here are CO_2 measurements recorded aboard two NASA research aircraft during the TRACE-P expedition. These observations were made in late winter/early spring when the eastward transport of air masses originating over the Asian continent peaks and during a neutral to weak La Nina period. In the following text, we use these data to elucidate the horizontal and vertical variations of CO_2 throughout the tropospheric column. We then examine the chemical relationships of several gases to establish outflow characteristics and backward trajectories coupled with an emissions inventory to deduce source regions. The final section describes CO_2 flux estimates for Asia derived from the in situ data.

2. Experiment

2.1. Study Region

[5] The airborne component of TRACE-P was conducted using the NASA Dryden DC-8 and Wallops P-3B research aircraft instrumented for in situ and remote measurements of an extensive suite of trace gases and aerosols. Initially, the mission progressed through the tropical North Pacific with flights transiting from Hawaii, Wake Island, and Guam prior to reaching East Asia. Eighteen sorties were flown out of intensive operational sites located in Hong Kong, China (7 March–13 March) and Yokota Air Force base in Fussa, Japan (21 March–2 April). Flights had an average duration

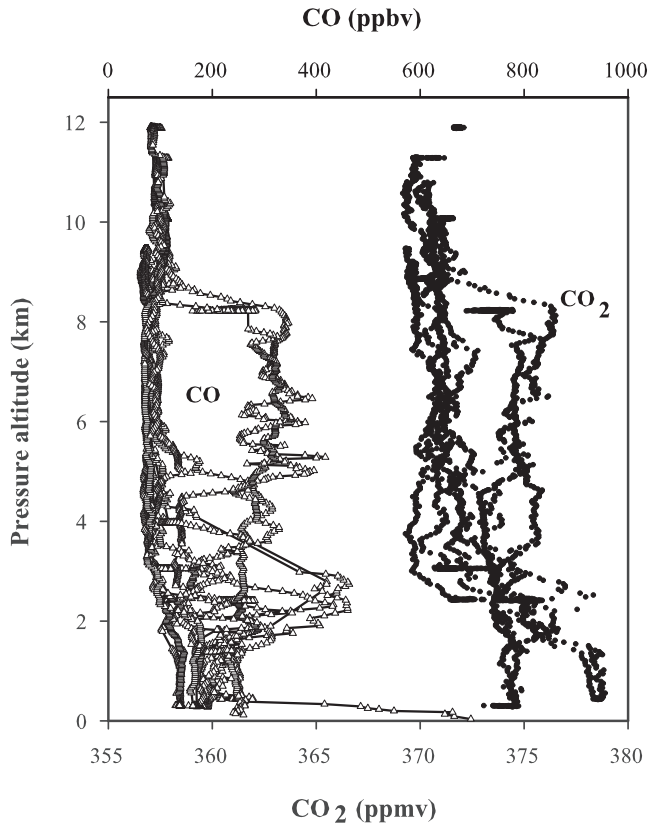

Figure 2. Vertical distribution of the mixing ratios of CO_2 and CO illustrating outflow observed below 8 km during the first local flight out of Hong Kong on 7 March 2001.

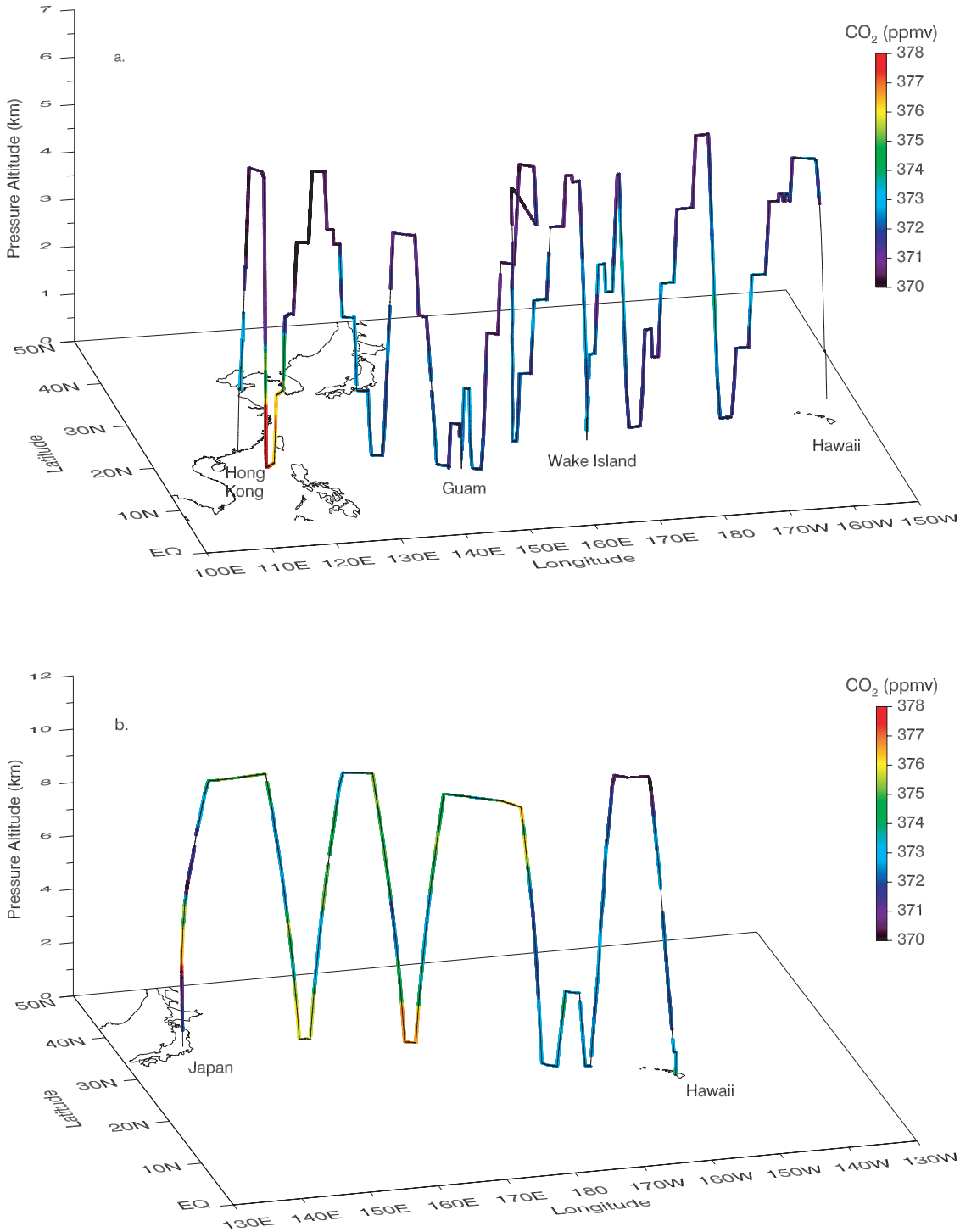

Figure 3. CO_2 concentrations observed on TRACE-P transit flights (a) P-3B progression from Kona, Hawaii to Wake Island (2/27/01), Wake Island to Guam (3/1/01), and Guam to Hong Kong, China (3/4/01) (b) DC-8 flight from Fussa, Japan to Kona, Hawaii (4/3/01).

of 8 hours and covered the altitude range of 0.3 km to 12.8 km. This paper focuses on data obtained near the Pacific Rim over the geographic area encompassing 5°–45°N latitude and 110°–160°E longitude. Data acquired on transit flights are also utilized in this analysis. A map of the study area is provided in an overview paper describing the scientific rationale of the mission and specifics of individual science flights [*Jacob et al.*, 2003]. Mean large-scale flow patterns along with transient synoptic scale features during TRACE-P are presented by *Fuelberg et al.* [2003].

2.2. Sampling Methodology

[6] Details of our experimental procedures have been described elsewhere [*Anderson et al.*, 1996; *Vay et al.*,

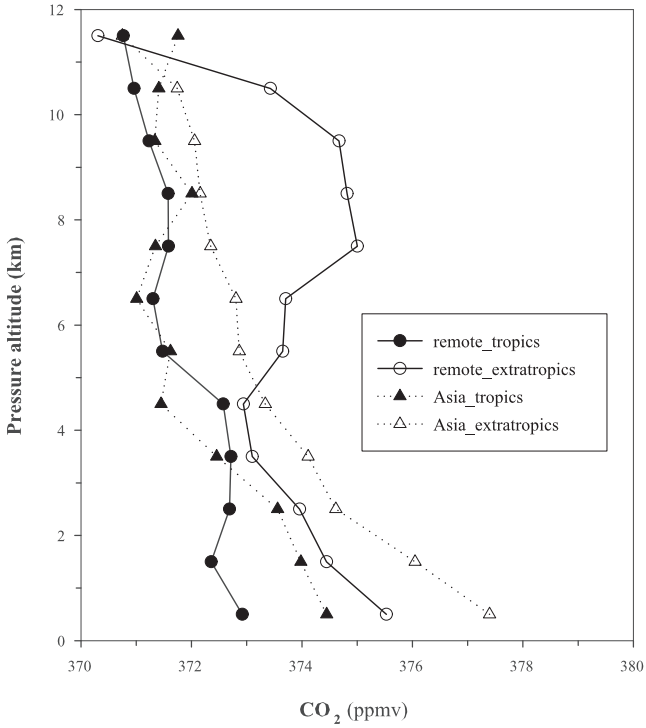

Figure 4. Comparisons of the mean CO_2 concentrations for the remote Pacific and near-Asia regional groups showing the overall higher mixing ratios in the extratropics most notably in the middle to upper troposphere several thousand kilometers downwind of the Asian continent.

1999]; therefore only a brief description is given here. In situ CO_2 measurements were made aboard both aircraft using modified Li-Cor model 6252 nondispersive infrared analyzers. During ambient sampling, air is continuously drawn through a Rosemount inlet probe, a permeable membrane dryer to remove $H_2O_{(v)}$, the Li-Cor, then through a diaphragm pump which vents overboard downstream of investigator's sampling inlets. The instruments are operated at a constant pressures, temperatures, and mass flows of 250 torr, 40°C, and 1000 cm^3 min^{-1}, respectively. Calibrations are performed at approximately 15-min intervals using standards obtained from the National Oceanic and Atmospheric Administration/Climate Monitoring and Diagnostics Laboratory (NOAA/CMDL). The CO_2 mixing ratios assigned to these standards are directly traceable to the World Meteorological Organization (WMO) primary calibration standards maintained at the CMDL laboratory in Boulder, Colorado. Data were recorded at 0.2 s (DC-8) and 0.02 s (P-3B), averaged to 1 s intervals, and have a precision (1σ) of 0.070 ppmv and an accuracy of ±0.2 ppmv.

[7] Surface data from NOAA/CMDL [*Komhyr et al.*, 1983; *Conway et al.*, 1994] and the Japan Meteorological Agency (JMA) [*Watanabe et al.*, 2000] are employed for purposes of examining ground-based CO_2 measurements in conjunction with those obtained aloft. All CO_2 surface measurements used in this study are traceable to the WMO scale. In addition to the CO_2 data, we present information on several other important trace gases including carbon monoxide (CO), ethane (C_2H_6), ethene (C_2H_4), ethyne (C_2H_2), propane (C_3H_8), perchloroethylene (C_2Cl_4), and methyl chloride (CH_3Cl). Specifics regarding the measurement of CO and the nonmethane hydrocarbons (NMHCs) and halocarbons are described in earlier papers by *Sachse et al.* [1988] and *Blake et al.* [1996], respectively.

3. Regional Distribution of CO_2

[8] Figure 1 summarizes the results of the airborne CO_2 measurements obtained during TRACE-P over the western North Pacific basin. The data, plotted as the averages for 1° latitude by 1° longitude bins, are for the altitude bands 0–2 km, 2–8 km, and 8–12 km. These breaks in the vertical distribution were chosen based on planetary boundary layer heights (PBL) and the observation that continental outflow occurred predominately below 8 km (Figure 2). The large-scale distribution of CO_2 shows that the highest mixing ratios were recorded in the extratropics below 2 km near the Asian continent. Significant differences between the near-surface and upper tropospheric CO_2 concentrations are also evident as well as a longitudinal inhomogeneity in the spatial distributions of CO_2.

[9] Other important features illustrated in Figure 1 are the variability of CO_2 concentrations over very narrow latitude ranges and the less pronounced meridional gradients in the upper troposphere (UT) relative to the surface. Lower CO_2 mixing ratios were observed in the tropics than in the northern extratropics except in the UT where similar concentrations were measured. Examination of the tropical data obtained during the P-3B westward transit flights from Hawaii to Hong Kong (Figure 3a) reveals a fairly uniform distribution for CO_2 over the remote Pacific where northeasterly trade winds prevailed. Approaching Hong Kong, however, CO_2 mixing ratios are notably enhanced when sampling Asian outflow advected over the South China Sea by the northeasterly winds of the continental high that dominates in winter. In contrast to the tropical observations, Figure 3b illustrates the influence of Asian emissions on the CO_2 spatial distributions observed over the remote extra-

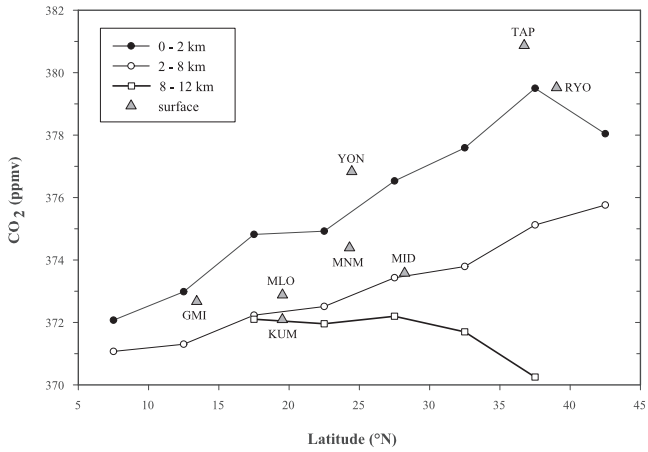

Figure 5. Latitudinal distribution of the mixing ratio of CO_2 over the western North Pacific shown in conjunction with surface data from monitoring stations operated throughout the North Pacific by the JMA and NOAA/CMDL.

Table 1. NOAA/CMDL and JMA Surface Station Information and Statistics for March 2001 Surface Data

Station Code	Station	Latitude, °N	Longitude	Sampling Frequency[a]	Mean, ppmv	±1 σ, ppmv	Median, ppmv	N
GMI	Guam, USA	13.43	144.78°E	weekly	372.67	0.87	372.29	17
KUM	Cape Kumukahi, USA	19.52	154.82°W	weekly	372.09	0.66	371.77	6
MID	Midway, USA	28.22	177.37°W	weekly	373.58	1.05	373.47	10
MLO	Mauna Loa, USA	19.53	155.58°W	weekly	372.88	0.27	372.93	15
MNM	Minamitorishima, Japan	24.30	153.96°E	continuous	374.39	0.85	374.33	666
RYO	Ryori, Japan	39.03	141.83°E	continuous	379.52	2.38	379.19	744
TAP	Tae-ahn Peninsula, Rep. of Korea	36.73	126.13°E	weekly	380.87	1.23	381.25	14
YON	Yonagunijima, Japan	24.46	123.02°E	continuous	376.83	2.16	376.47	714

[a]Statistics for JMA data calculated from hourly averages.

tropical Pacific during the DC-8 transit flight from Japan to Hawaii.

3.1. Vertical Gradients Over the Remote Pacific and Near-Asia Regions

[10] The temporal coverage of the TRACE-P expedition roughly coincided with the maximum of the CO_2 seasonal cycle occurring on the Earth's surface. North of the tropics, extrema occur in March–April at the surface [*Conway et al.*, 1988, 1994; *Watanabe et al.*, 2000] and in early May in the lower troposphere [*Tanaka et al.*, 1983]. In the Northern Hemispheric winter, CO_2 is fairly uniform in the mixed layer and generally exhibits a decreasing trend with height above the PBL [*Tanaka et al.*, 1983]. This strong negative vertical mixing ratio gradient is attributable to reduced photosynthetic activity, the rapid mixing in the PBL of CO_2 released from respiration (plants, soil, animals, humans) and combustion processes, and the suppression of mixing above this layer.

[11] To examine the regional differences of the vertical CO_2 profiles over the North Pacific, TRACE-P CO_2 data were separated into remote Pacific and near-Asia regional groups. These groups were then further divided into tropics (10°–23.5°N) and extratropics categories (23.5°–35°N); the division being based on the formal definition of the tropics as the 23.5° parallel. An upper geographic boundary of 35°N was used since sampling in the remote region did not extend beyond this latitude. The longitudinal range for each of the four regions is 110°–150° E (Asia tropics), 150°–205°E (remote tropics), 120°–160°E (Asia extratropics), and 160°–205°E (remote extratropics). A sliding longitudinal scale was invoked since the Asian continent extends further out into the Pacific at more northerly latitudes. From Figure 4 we see that during late winter/early spring, mean CO_2 values in the extratropics are about 6.5 ppmv higher near the surface than in the UT and that CO_2 concentrations can be highly variable even within the UT at locations far removed from surface sources. The influence of a greater concentration of surface sources in the mid-latitudes is reflected in the larger means for the extratropical regions. In contrast, the vertical gradients observed in the northern tropics exhibit little zonal variability changing only 2–3 ppmv over 12 km. These observations are consistent with previous measurements by *Nakazawa et al.* [1991] and *Anderson et al.* [1996] and result from the reduced significance of local CO_2 source/sink processes and the prevalence of rapid vertical transport in the tropical region.

[12] Higher mean CO_2 concentrations, apparent in the lower tropospheric data for both near-Asia regions, indicate the influence of sources on the Asian continent. Overall, a decreasing trend with height was observed except in the remote extratropical region. This may be attributable to the fact that the data comprising the 7–11 km altitude bins are from a single flight where Asian outflow was intercepted en route from Fussa, Japan to Kona, Hawaii (Figure 3b). However, the positive vertical mixing ratio gradient between 5 and 7 km was determined from data acquired on several different flights suggesting CO_2-enriched air parcels were sampled several thousand kilometers downwind of the Asian continent on more than one occasion. A general convergence of the means above 8 km reflects how the concentration of CO_2 can exhibit little variability over very large spatial scales.

3.2. Latitudinal Distribution

[13] The results from averaging the airborne CO_2 observations by latitude are shown in Figure 5 along with simultaneous surface measurements from several monitoring stations (Table 1) located throughout the TRACE-P sampling domain. The aircraft data, limited to the near-Asia region, are also summarized in Table 2. The latitudinal data exhibit several notable characteristics. For example, the increasing trend that progressed from the tropics to the mid-latitudes for mean CO_2 concentrations below 8 km. The regression of CO_2 with latitude (5°–40°N) was equally

Table 2. Statistics for Aircraft Measurements Presented in Figure 5

Latitude	Altitude, km	Mean, ppmv	±1 σ, ppmv	Median, ppmv	N
5°–10°N	0–2	372.07	0.74	372.23	640
	2–8	371.07	0.50	371.05	949
10°–15°N	0–2	372.98	1.09	372.48	388
	2–8	371.30	0.68	371.18	1018
15°–20°N	0–2	374.82	1.08	375.32	892
	2–8	372.23	1.08	371.88	2379
	8–12	372.10	0.67	371.94	1067
20°–25°N	0–2	374.92	1.75	375.05	8590
	2–8	372.51	1.48	372.29	16200
	8–12	371.96	1.34	371.67	6485
25°–30°N	0–2	376.53	2.42	376.35	7926
	2–8	373.43	1.34	373.37	9518
	8–12	372.20	1.27	372.34	3075
30°–35°N	0–2	377.59	1.89	377.39	10354
	2–8	373.79	1.57	373.37	13574
	8–12	371.70	1.60	372.09	2475
35°–40°N	0–2	379.50	4.34	378.82	7608
	2–8	375.12	2.05	374.81	10982
	8–12	370.25	1.83	369.02	523
40°–45°N	0–2	378.04	1.00	377.79	579
	2–8	375.76	1.37	375.83	1599

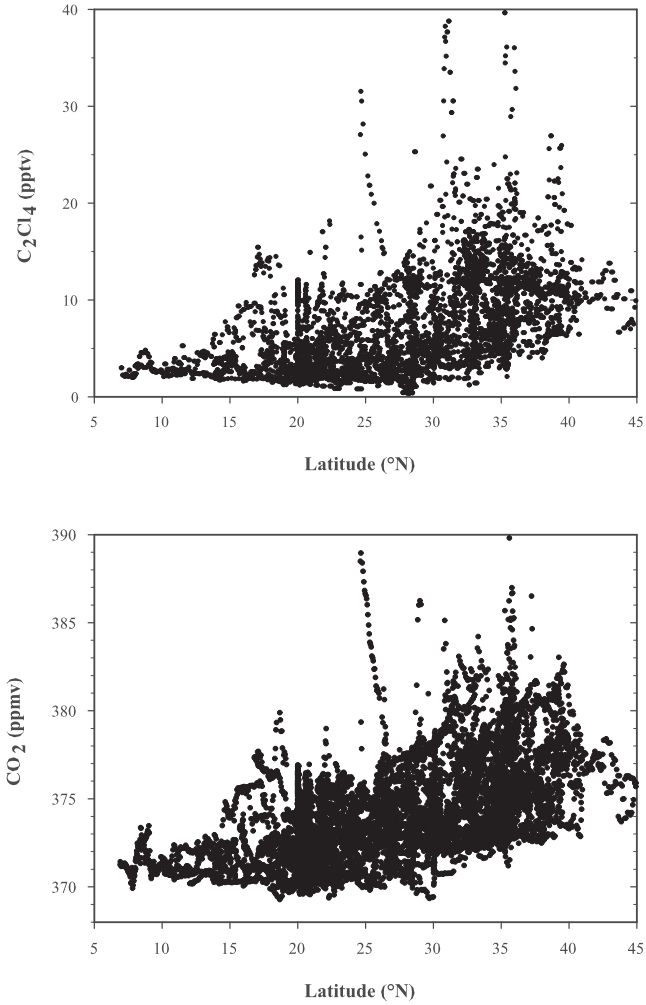

Figure 6. Latitudinal distribution of the mixing ratios of CO_2 and C_2Cl_4 for the near-Asia region. Coincident enhancements in these respective combustion and industrial tracers are suggestive of common sources.

strong (r^2 = 0.98) for the lower two altitude bins. Such a trend is expected for late winter/early spring, however, based on prior shipboard measurements over the western Pacific the highest mixing ratios would be anticipated at the most northern latitudes [*Nakazawa et al.*, 1992]. Here we see in both the aircraft and surface data indications of a band of maximum emissions (35°–40°N) presumably driven by the larger surface sources there. The variability evident in the surface data for this particular latitude range may reflect differences in geographic location (i.e., proximity to localized sources), sampling frequency, or data selection procedures.

[14] These data further demonstrate that CO_2 mixing ratios observed at surface stations located within the Pacific Rim region can be significantly higher than those measured at sites far removed from the influence of surface sources. Even though Minamitorishima (MNM) and Yonagunijima (YON) are located almost in the same latitude, a difference of about 2.4 ppmv was recorded between the two stations for March 2001 implying that Yonagunijima is susceptible to the Asian continent in winter [*Wantanabe et al.*, 2000]. Also noteworthy is a lower mean value for the more northern yet further downwind Midway Island station than for Minamitorishima. A similar trend is also apparent in the lower altitude aircraft data where differences of 3 ppmv are seen in some cases between the remote Pacific surface measurements and those obtained aloft in the PBL near-Asia.

[15] Another feature of interest is how the trend with latitude above the PBL is less pronounced than that observed at or near the surface. This is consistent with earlier aircraft measurements over Japan that showed the seasonal variation of CO_2 decreased with height above the ground and had a phase shift or lag between the LT and UT of about 1 month [*Tanaka et al.*, 1983]. Within the UT mean values are fairly uniform except for the mid-latitudinal data where the sampling of stratospherically influenced air parcels (O_3 > 100 ppbv) resulted in lower mean CO_2 concentrations. Examination of the lower stratospheric and UT data for the 35°–40° N latitude bin reveals mean CO_2 mixing ratios of 368.79 ppmv and 371.99 ppmv, respectively. Such stratospheric-tropospheric exchange processes are associated with upper tropospheric wave breaking at the Japan Jet [*Austin and Midgley*, 1994] which exhibited peak mean speeds of 50–65 ms^{-1} at 300 hPa near Japan during Trace-P [*Fuelberg et al.*, 2003].

4. Characterization of Outflow

[16] The distribution patterns of NMHCs, halocarbons, CO, and CO_2 can be used to characterize anthropogenic sources such as incomplete combustion and industrial activity. For example, elevated concentrations of C_2H_6, C_2H_4, and CO_2 are associated with combustion activities, whereas C_2Cl_4 is released exclusively by industrial processes [*Blake et al.*, 1996, 1997]. Since the sources of these atmospheric trace species are predominately land-based, the impact of continental emissions on air masses can be assessed by the observed changes in their mixing ratios. During TRACE-P, the latitudinal distributions of C_2Cl_4 and CO_2 shown in Figure 6 illustrate that air parcels over the western North Pacific were frequently augmented with chemical compounds originating from anthropogenic activities. Evidence of common sources is apparent in the coincident enhancements of these two tracers north of 17°N, particularly in the extratropics where the highest mixing ratios were measured.

[17] While CO is a general indicator of combustion, this is the only known source of C_2H_2 [*Singh and Zimmerman*, 1992; *Talbot et al.*, 1997]. C_2H_2 is removed from the atmosphere approximately 3 times faster than CO via the reaction with OH thus the photochemical aging of an air mass postemission leads to a decreasing C_2H_2/CO ratio. Prior studies have demonstrated that this ratio can be used as an indicator of the relative degree that air masses have been processed by the combined actions of atmospheric mixing and photochemistry [*McKeen and Liu*, 1993; *McKeen et al.*, 1996; *Smyth et al.*, 1996, 1999].

[18] After *Smyth et al.* [1996, 1999] we use the C_2H_2/CO ratio as a measure of the degree of atmospheric processing to study the distribution and budget for CO_2 as observed during TRACE-P. The relationship between C_2H_2 and CO is utilized as a surrogate ordinate for examining the functional

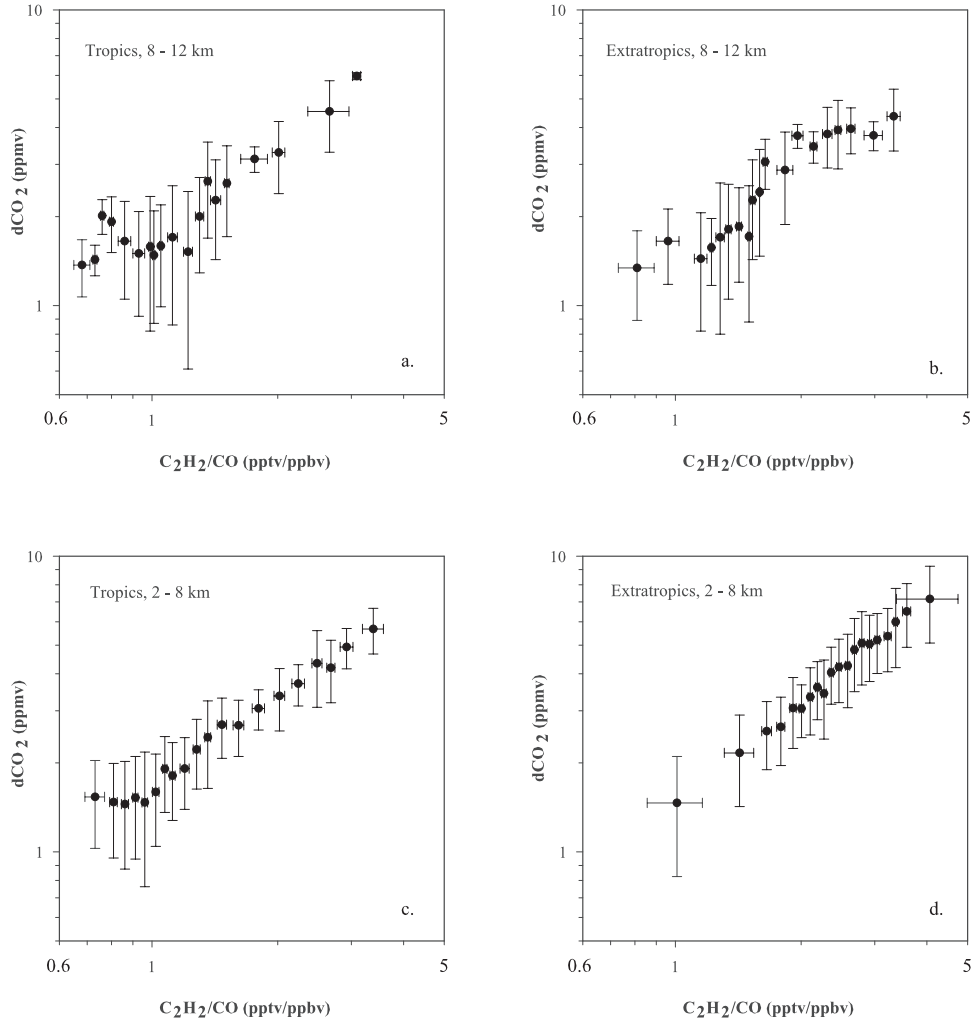

Figure 7. Aggregate means for dCO_2 and the ratio of C_2H_2/CO illustrating the degree of atmospheric processing of combustion-related emissions in the free troposphere for (a) Tropics, 8–12 km (b) Extratropics, 8–12 km (c) Tropics, 2–8 km, (d) Extratropics, 2–8 km.

dependence of CO_2 relative to the degree that the atmosphere has processed emissions from combustion sources. Data obtained in the near-Asia region were initially filtered to remove any stratospheric influence (O_3 >100 ppbv) then the lowest CO_2 mixing ratio (369.5 ppmv) within this subset of tropospheric values was subtracted from the remaining measurements to accentuate trends in the data (ΔCO_2). These data were then formed into aggregates, each containing 5% of the CO_2 measurements, and the mean for each aggregate calculated (i.e., aggregate means). The results for the near-Asia tropics and extratropics regions are illustrated in Figures 7a–7d where the error bars indicate ±1 σ about the means.

[19] The correlative relationship between CO_2 and C_2H_2/CO is quite robust ($r^2 > 0.97$) for ratios >1 except in the extratropical UT ($r^2 = 0.83$) reflecting less impact from fresh surface emissions on these upper tropospheric air parcels (Figure 7b). The highest dCO_2 values and largest C_2H_2/CO ratios were observed below 8 km within the extratropics (Figure 7d), indicating the injection of fresher continental combustion-related emissions into the atmosphere overlying this region. Apparent differences in the aggregate distribution patterns (i.e., majority of aggregate means having ratios >2 and none with ratios <1) further reveal that air masses sampled in the extratropical lower free troposphere were the least processed via mixing and chemistry.

[20] Also notable are the higher CO_2 mixing ratios in the tropical UT compared with upper tropospheric values observed further north. The plateau in CO_2 for C_2H_2/CO mixing ratios >2 (Figure 7b) is suggestive of the influence

Table 3. Covariance of CO With Respect to CO_2, Selected NMHCs and Halocarbons Expressed as r^2 for the Near-Asia Region UT

Species	Source	Tropics (13.9°–23.5°N)	Extratropics (23.5°–35.6°N)
CO_2	Combustion, biogenic	0.77	0.68
C_2H_6	Combustion/fuel	0.94	0.82
C_2H_4	Combustion	0.73	0.64
C_2H_2	Combustion/fuel	0.93	0.87
C_3H_8	Combustion/fuel	0.86	0.67
C_2Cl_4	Industrial	0.75	0.36
CH_3Cl	Biomass burning, marine	0.60	0.69

Table 4. Summary for the 11 Pollution Plumes Sampled With CO_2 Mixing Ratios in Excess of 380 ppmv[a]

Flight, date	Max CO_2, ppmv	Max C_2Cl_4, pptv	Max C_2H_2, pptv	Max C_2H_4, pptv	Height of Tracer Max, PBL, km	Trajectory Sector (Origin Listed First)	Meteorology
D_09, 3/10	382.13	24	2124	811	0.6, 0.8	WNW/W	ahead of front
D_09, 3/10	381.74	12	1205	648	0.5, 0.65	NW, WNW/W	behind front
D_09, 3/10	382.79	23	2186	752	0.9, 0.95	WNW/W	crossed front
D_12, 3/18	389.67	16	1261	1822	0.38, 1.4 → 0.8	WNW/W	behind front
D_13, 3/21	393.64	123	10403	3052	0.34, 0.85 → 0.65	WNW/W	behind front
P_13, 3/17	384.53	25	2415	871	1.45, 1.5	tropics and WNW/W	behind front
P_13, 3/17	386.22	24	2440	901	1.55, 2.0	tropics and WNW/W	behind front
P_14, 3/18	388.55	22	3059	1499	0.12, 1.3	WNW/W	behind front
P_19, 4/2	383.99	26	1232	416	0.63, 1.4	N/NE, NW, WNW/W	ahead of front
P_19, 4/2	382.20	26	1240	786	0.23, 1.4	N/NE, NW, WNW/W	ahead of front
P_19, 4/2	383.06	19	978	159	0.22, 2.1	N/NE, NW, WNW/W	crossed front

[a]Representative March surface "background" concentrations for C_2Cl_4, C_2H_2, and C_2H_4 in the midlatitudes are approximately 11 pptv, 500 pptv, and 10 pptv, respectively.

of variable source emission ratios of CO_2 relative to those of C_2H_2 and CO [*Smyth et al.*, 1996]. Indeed, the relationship between mixing ratios of CO and selected NMHCs and halocarbons reveals a different apportionment of sources for the two regions (Table 3). Particularly noteworthy is the overall higher correlation with CO for selected gases in the tropics category and the absence of a strong industrial signature at more northerly latitudes. Some of the air parcels encountered by the aircraft in the tropical UT originated deep within the tropics or over equatorial Africa which were regions of abundant precipitation and lightning [*Fuelberg et al.*, 2003]. Furthermore, TRACE-P occurred during the peak of the biomass burning season in Southeast Asia [*Liu et al.*, 1999] and enhancements in CO_2 mixing ratios attributable to biomass burning in this region have been reported from prior aircraft measurements in the UT during El Nino years [*Matsueda and Inoue*, 1999; *Matsueda et al.*, 2002]. Thus long-range transport from these highly convective areas at the height of the burning season likely contributed to the observed differences in upper tropospheric CO_2 concentrations.

[21] The nonlinearity at the lowest C_2H_2/CO ratios suggests that some limiting value is reached that is representative of a background mixing ratio [*Smyth et al.*, 1996]. If the $\pm 1\sigma$ variability about the means is considered, a background CO_2 concentration of approximately 372 ppmv is then implied for the near-Asia domain. From the data presented in Figure 7, we conclude that continental outflow was more efficient below 8 km between 23.5° and 45°N and that combustion processes occurring within this region were a significant source of CO_2 to the atmosphere in late winter/early spring of 2001.

5. Source Regions

[22] Eleven pollution plumes having CO_2 and CO mixing ratios in excess of 380 ppmv and 250 ppbv, respectively, were identified in the data set. The selection criterion for CO_2 was based on the highest mean value observed in the aircraft data presented in Figure 5. The close correspondence between the means for the aircraft and continuous Ryori surface measurements (379.50 versus 379.52 ppmv) gives high confidence in using 380 ppmv as a filter for a CO_2 concentration in excess of that attributable to the seasonal mean between 35° and 40°N. All the plumes were intercepted in the extratropics (>24.57°N) near the Asian continent within the PBL (PBL height range: 0.7–2.1 km). PBL heights were determined by examining virtual potential temperature, water vapor, and vertical wind signatures [*Thornhill et al.*, 2003] during descents to and ascents from boundary layer runs.

[23] In winter, cold surface temperatures over extratropical Asia create a stable low-level inversion that inhibits the venting of pollution out of the PBL [*Yienger et al.*, 2000]. During late winter/early spring, cyclogenesis increases and these low-pressure baroclinic systems provide an uplifting mechanism by which continental emissions are lofted above the surface by strong winds in the dry air behind a cold front [*Ing*, 1972; *Merrill et al.*, 1985; *Chen et al.*, 1991]. Indeed, the 11 pollution events encountered during the mission were all associated with frontal activity (D. J. Westberg, personal communication), and *Liu et al.* [2003] have demonstrated that transport in the PBL behind cold fronts was a major process driving Asian pollution outflow during the TRACE-P period. Discrete plumes sampled behind cold fronts were more highly enriched in CO_2 than those probed ahead of or while crossing the fronts (Table 4). A combustion influence, most of which is clearly anthropogenic in origin owing to coincident enhancements in C_2Cl_4, is evident given the significant covariance CO_2 mixing ratios exhibit with respect to CO ($r^2 \geq 0.89$). Furthermore, evidence of the "freshness" of the emissions is apparent in the elevated concentrations of C_2H_4 ($\tau \sim 2$ days).

[24] Five-day backward trajectories coupled with a trajectory classification scheme and a CO_2 emissions database developed for Asia were employed in this analysis to deduce source regions. Trajectories utilized global-gridded meteorological analyses prepared by the European Centre for Medium-Range Weather Forecasts (ECMWF). The 5-day backward trajectories were calculated using a kinematic model [*Fuelberg et al.*, 2003]. Trajectories arriving at the various altitudes of the aircraft during flight were used here.

[25] The emissions database for CO_2 was estimated as a part of the overall TRACE-P Asian emissions inventory [*Streets et al.*, 2003]. It is designed to cover 13°S to 53°N in latitude and 60°–157°E in longitude and it includes 22 Asian countries, 60 subregions, and 115 active large point sources (LPSs). The estimated total CO_2 emissions in Asia for the year 2000 are 2693 Tg C yr^{-1}. Included source sectors and their fractions (percent of total emission) are

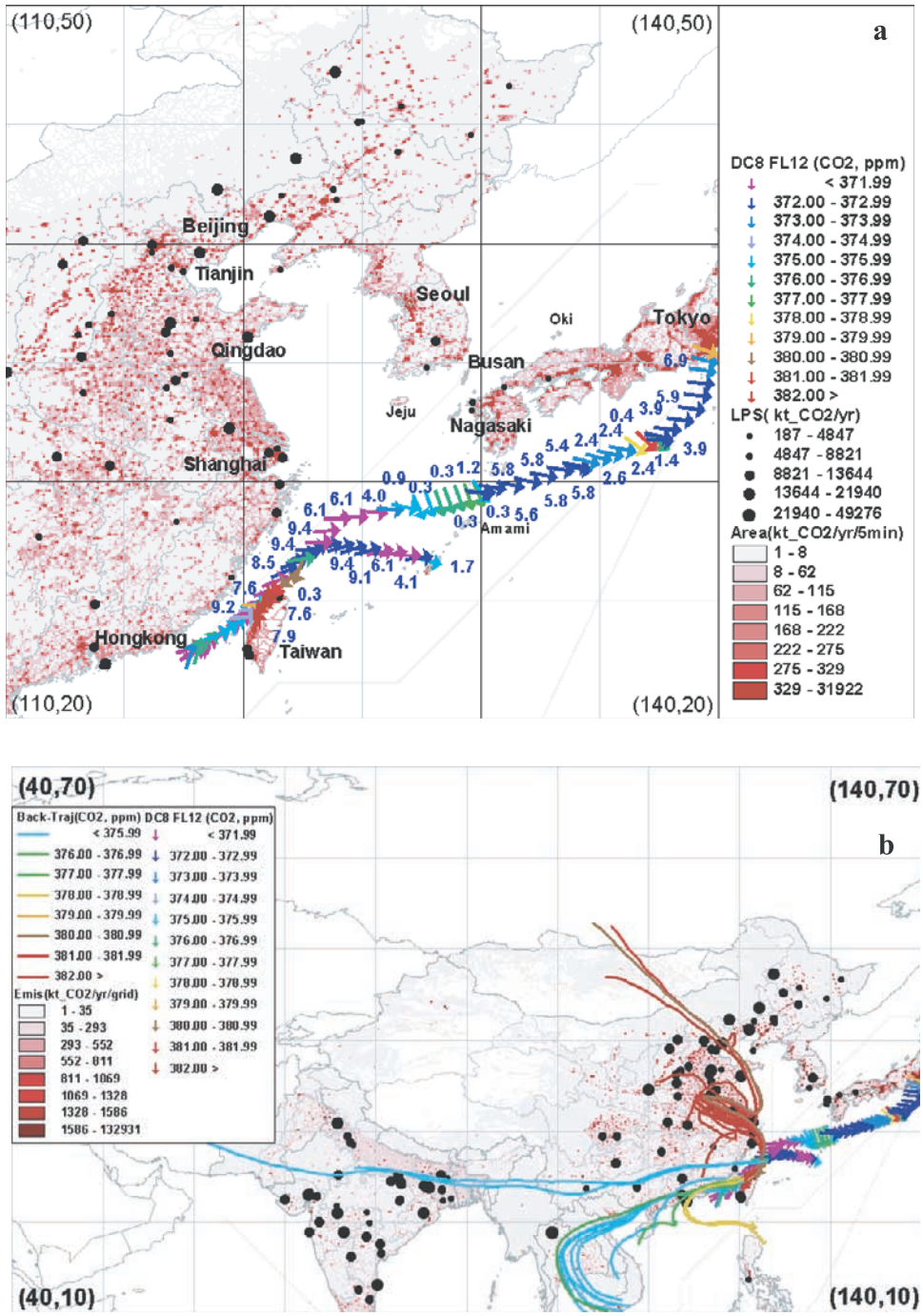

Figure 8. CO_2 emissions database for Asia for the year 2000 and data associated with the pollution plume intercepted in the Taiwan Strait having a CO_2 enhancement of 389.6 ppmv (a) CO_2 mixing ratios depicted along the 18 March 2001 flight track superimposed on the emissions map. The colored arrows illustrate the CO_2 mixing ratio and wind direction, whereas the numbers along the flight track are for the DC-8 altitude in kilometers. LPS represents large point sources. (b) Backward 5-day trajectories for the boundary layer run in the Taiwan Strait illustrating the lower CO_2 concentration associated with the southwest flow above the front and the higher concentrations observed below the front when northeasterly flow emanating from the high emissions area of Shanghai was sampled.

industry (23%), domestic (6%), transportation (11%), power generation (23%), cement production (3%), biofuel combustion (22%), and biomass burning (12%). Uptake from growing vegetation is not included. In the work of *Streets et al.* [2003], estimated CO_2 releases from this study were compared with recent IPCC estimates [*Nakicenovic and Swart*, 2000] for anthropogenic source sectors (without the inclusion of open biomass burning but including biofuels) and were 2382 Tg C yr^{-1} and 2030 Tg C yr^{-1}, respectively.

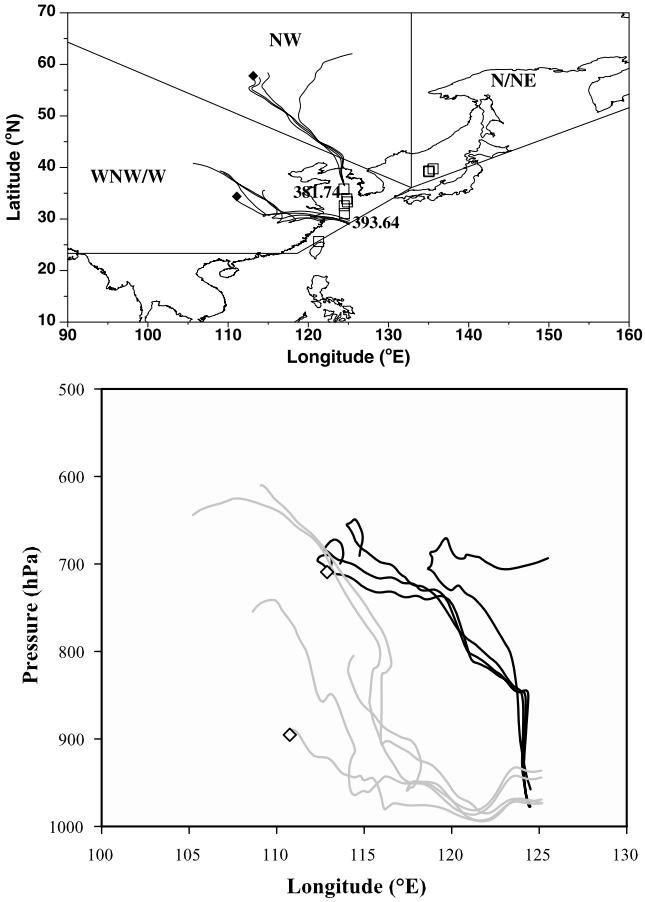

Figure 9. Example of the trajectory analyses utilized to identify source regions (a) Sector classification invoked shown along with 5-day backward trajectories for the pollution plumes having the largest and smallest CO_2 enhancements. Open square symbols depict the location of the 9 other plumes. (b) trajectory heights for the plume having a maximum CO_2 mixing ratio of 393.64 ppmv shown in grey and in black for the plume with the smallest enhancement of 381.74 ppmv. Origin of trajectories associated with these concentrations shown with diamond symbol.

[26] For our study we used a gridded CO_2 database with a multispatial resolution gridding methodology developed from other researchers [*Streets et al.*, 2003; *Woo et al.*, 2003]. This methodology can generate gridded CO_2 emission data from 30 × 30 arc-second to the any lower resolution grid using various types of Geographic Information System/Remote Sensing datasets. A 5 × 5 minute grid resolution CO_2 emissions data was used for this analysis. In terms of the spatial distribution of the sources, industrialized regions/countries in East Asia (central and east provinces of China, South Korea, Japan, Taiwan) show higher emissions intensity owing to the larger fraction of industrial, power generation, and transportation sectors located there compared with Southeast Asian countries that have a relatively lower level of emissions.

[27] Figure 8a provides an example of the emissions database for Asia with the DC-8 flight track for 18 March 2001 also shown. The DC-8 departed from Okinawa, flew to the southern end of the Taiwan Strait, and on the return leg spiraled down into the PBL (1.4 km) at the NW tip of Taiwan. The front was penetrated at ~1 km while descending to 0.3 km for the boundary layer run. Winds were from the southwest above the front and from the northeast below it. The backward trajectories, which document the history of the air parcels sampled by the aircraft for this particular flight segment, are depicted in Figure 8b. Each trajectory shown is color-coded to represent the associated CO_2 concentration. Here we see that the air parcel sampled above the front (CO_2 < 378 ppmv) mostly originated over the Indian subcontinent and Southeast Asia. Below the front, the backward trajectories indicate that the air mass had been advected from the industrialized coastal region near Shanghai where large CO_2 sources are indicated on the emissions map. Examination of the trajectory heights shows this air parcel originated at about 950 hPa, descended to the near surface, then ascended to 800 hPa prior to interception.

[28] The sector classification invoked here for the trajectory analysis is based on the prior work of *Pochanart et al.* [1999]. In this scheme, East Asia is subdivided into three regions that are representative of the various types of air masses observed at Oki, Japan namely the N/NE (background Eurasian continental or cleanest), NW (background continental slightly perturbed by anthropogenic activity), and WNW/W (regionally polluted). For example, the sectors along with the backward trajectories and trajectory heights for the most highly enriched (393.64 ppmv) and least augmented (381.74 ppmv) of the 11 pollution plumes are illustrated in Figure 9. From the figure we see that the largest pollution event was associated with an air mass that originated and stayed within the WNW/W sector the entire time traveling east over Shanghai. The air parcel remained below 900 hPa while traveling over some 1100 kilometers. In contrast, the smallest of the CO_2 plume enhancements is attributable to a continental air mass with its origin in the NW sector near Lake Baikal that had no near-surface contact.

[29] Examination of the plume-associated backward trajectories revealed that all were continental in origin except three that were briefly over the South China Sea prior to taking the WNW/W route over southeastern China. The highest CO_2 mixing ratios were observed in plumes resulting from air masses that stayed in the boundary layer for longer periods of time within the WNW/W sector where the predominance of the anthropogenic CO_2 emissions occur according to the database for Asia. Here 65% of the trajectories originated and were confined to the WNW/W region, 22% originated in the NW, 3% originated in the N/NE, and 11% originated in the Tropics. Every trajectory eventually passed through the WNW/W sector regardless of origin. Trajectory heights indicated that near-surface contact (>900 hPa) of the air parcels was frequently over large urbanized areas such as the coastal cities of Shanghai, Hong Kong, and Qingdao. Polluted air masses intercepted over the Sea of Japan came in close contact with the surface as they passed over Korea. Thus we conclude that the observed CO_2 enhancements in the eleven plumes were attributable to anthropogenic activities in northeast Asia and that the transport of these polluted

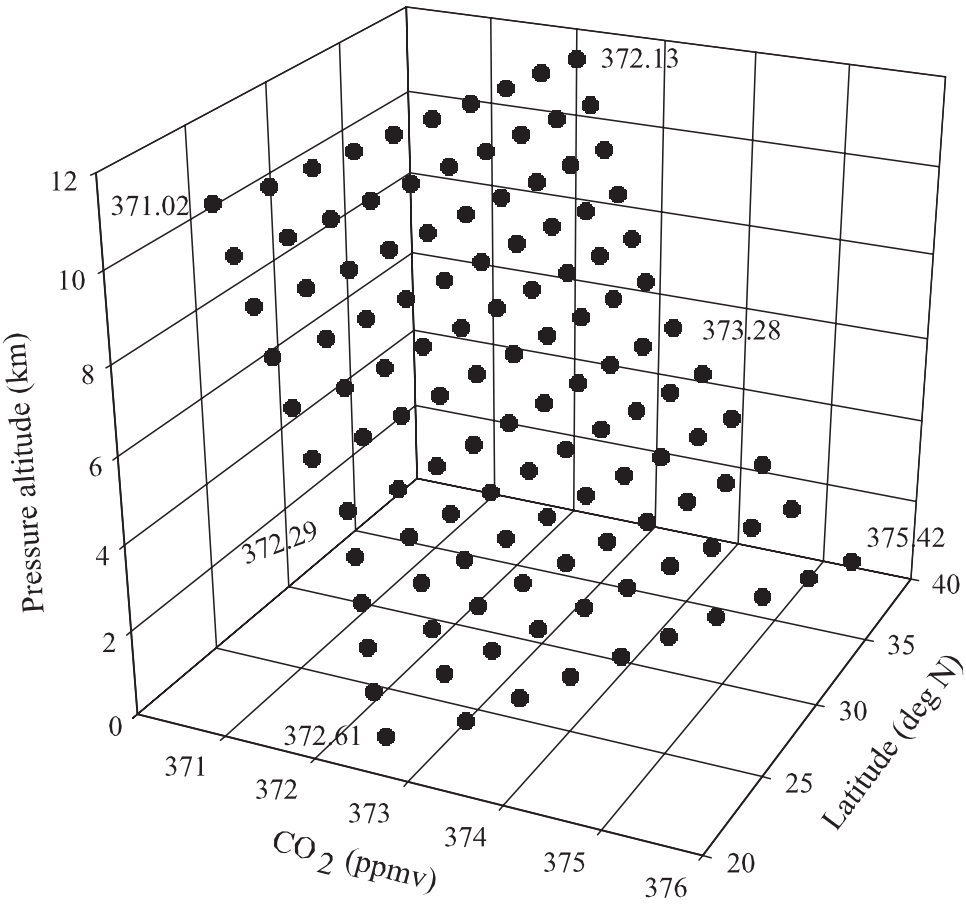

Figure 10. Latitude-altitude grid of variable background CO_2 mixing ratios calculated for the flux estimates. Indicated adjacent to the plot are the median CO_2 mixing ratios for the tropics remote and extratropics remote 0–2 km, 2–8 km, and 8–12 km altitude bins utilized to initialize the grid calculation.

air parcels from this source region was triggered by the episodic passage of cold fronts.

6. Export of CO_2 From the Asian Continent

[30] To explore the eastward flux of CO_2, data obtained within a box extending from 0 to12 km, 20° to 40°N latitude, and 120° to 150°E longitude were used to calculate a 1 km altitude by 2° latitude resolution, North-South grid of average CO_2, vector winds, and air density values. After subtracting a representative background level from the CO_2 values, fluxes were calculated for each grid point by taking the product of the average East-West wind vector and the corresponding density-corrected, CO_2 concentration enhancement. Zonal fluxes were determined by summing the grid-point values over the 12 × 10 grid. Carbon fluxes are the product of the total CO_2 flux times the molar fraction of carbon in CO_2.

[31] Two approaches were taken in determining the CO_2 background for purposes of constraining the estimated fluxes. As discussed in the Characterization of Outflow Section, the nonlinearity at the lowest C_2H_2/CO ratios implied that some limiting value was reached that was representative of a background mixing ratio which our analysis indicates is 372 ppmv. Calculations utilizing this average value thus provide an upper limit on the estimated net flux. The second approach entailed calculating a grid of background values for the spatial domain of the flux box based on median values observed within the remote tropics and remote extratropics for the 0–2 km, 2–8 km, 8–12 km altitude bins. Median values were then assigned latitudes of 20°N (remote tropics) and 40°N (remote extratropics) and altitudes of 0.5 km (0–2 km), 5.5 km (2–8 km), and 12 km (8–12 km) and a linear interpolation performed between these initial values. The resulting grid of background mixing ratios (Figure 10) thus accounts for the seasonal variation in CO_2 mixing ratio as a function of latitude and altitude.

[32] The results from these flux calculations are illustrated in Figure 11a and show that a significant component of the CO_2 export occurred below 10 km in the midlatitudes, most notably between 35° and 40°N. These data further indicate a negative flux within portions of the extratropical UT. Close examination of the average vector winds reveals higher speeds in the free troposphere with maximum velocities above 10 km (Figure 11b). As mentioned earlier, the core of the jet stream was positioned near Japan during TRACE-P with peak mean speeds at heights of ≤300 hPa [*Fuelberg et al.*, 2003] and was influential on upper tropospheric CO_2 distributions. These data suggest that such dynamical processes are important mechanisms for reducing the export of CO_2 from the region via dilution with stratospheric air containing lower CO_2 mixing ratios.

[33] In summing over the entire grid, we estimated a net CO_2 flux from the Asian continent of 13.93 Tg C day^{-1}

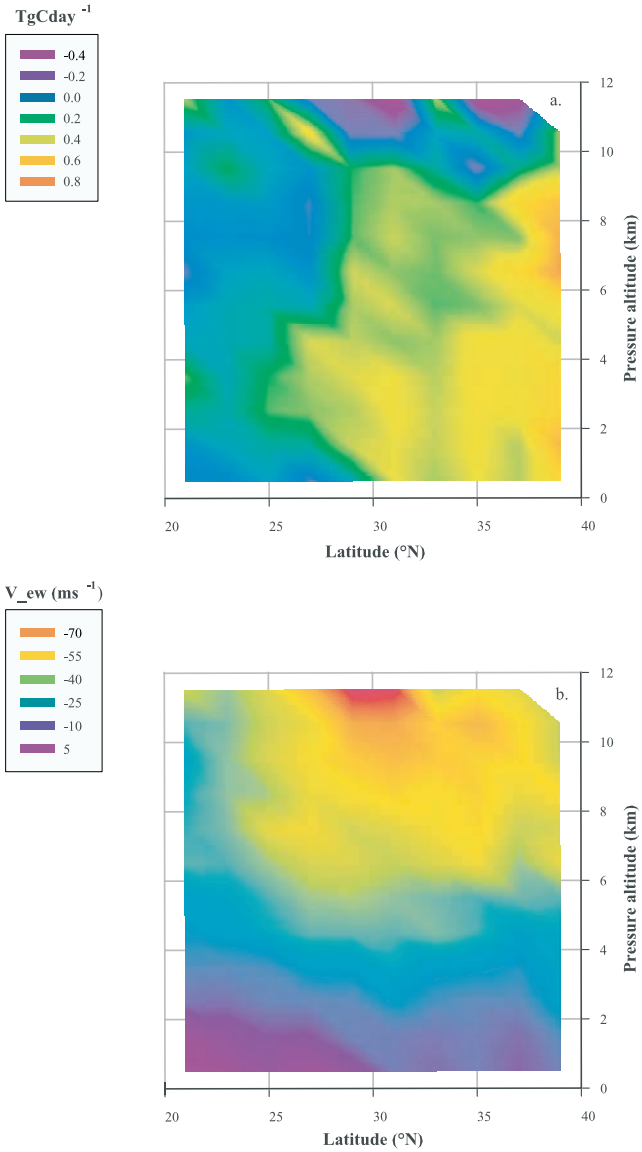

Figure 11. Latitude-altitude plots for the near-Asia region of (a) the CO_2 flux in Tg C day^{-1} and (b) average east-west wind velocities.

attributable to both natural and anthropogenic sources. The apportionment of the flux was 3.13 Tg C day^{-1} (22.5%), 11.0 Tg C day^{-1} (78.8%), and −0.18 Tg C day^{-1} (−1.29%) for the PBL, lower to middle troposphere (L-MT), and UT, respectively utilizing 372 ppmv as the background value. Further division of the 8–12 km bin shows a contribution of 1.65 Tg C day^{-1} (11.82%) for 8–10 km and a negative flux of −1.83 Tg C day^{-1} (−13.13%) for the uppermost 2 km. The finding that the majority of the CO_2 flux emanated from the lower free troposphere is consistent with our earlier results showing that continental outflow was more efficient between 2 and 8 km based on the relationship of dCO_2 to C_2H_2/CO.

[34] Invoking the background grid approach yielded a flux of 6.37 Tg C day^{-1} having a greater apportionment of the exported flux within the PBL (1.83 Tg C day^{-1} or 28.79%), 4.43 Tg C day^{-1} (69.62%) in the L-MT, and 0.10 Tg C day^{-1} (1.59%) in the UT. Fluxes of 1.31 Tg C day^{-1} (20.53%) and −1.21 Tg C day^{-1} (−18.94%) were observed for the 8–10 km and 10–12 km altitude bins, respectively. Since the gridded background values represent the contribution from the CO_2 seasonal cycle, and in the northern middle to high latitudes the terrestrial biosphere accounts for nearly the entire atmospheric CO_2 seasonal signal [*Fung et al.*, 1987; *Hunt et al.*, 1996], the lower constraint (6.37 Tg C day^{-1}) thus provides an approximation of the anthropogenic component of the observed flux. For comparison with our estimate from anthropogenic sources, a 1987 inventory of CO_2 emissions resulting from fuel combustion and industrial activities in Asia yielded 4 Tg C day^{-1} with 35°–40°N indicated as the band of maximum emissions [*Akimoto et al.*, 1994]. A more recent estimate for the year 2000 shows an emissions rate of 7.37 Tg C day^{-1} for an inventory based on direct combustion from anthropogenic sources including biomass burning [*Streets et al.*, 2003]. In comparing these estimates, however, consideration must be given to the fact that the TRACE-P CO_2 fluxes were determined primarily for March near the seasonal CO_2 maximum in a period characterized by enhanced Asian outflow, whereas the daily inventory estimates were averages calculated from an annual mean. Therefore seasonal imbalances in the CO_2 fluxes are not reflected in the inventory estimates presented here.

[35] Contributions to the overall net flux from biogenic sources, such as autotrophic and heterotrophic respiration, can also be inferred from these data. By looking at the difference between the overall net flux and the anthropogenic source contribution, these data reveal an overall biospheric flux of 7.56 Tg C day^{-1} or approximately 54% of the total net flux (i.e., 13.93 Tg C day^{-1} – 6.37 Tg C day^{-1} = overall biospheric flux or 7.56 Tg C day^{-1}). By comparison, fluxes constrained by stations in the South China Sea were estimated at 2.19 Tg C day^{-1} for Tropical Asia (20°S–20°N) using an atmospheric transport model and inverse modeling [*Ciais et al.*, 2000]. To the best of our knowledge, this is the only recent estimate available in the current literature of an overall biospheric flux constrained by observations obtained near the Asian continent. Our higher estimate could be attributable to several factors including: our spatial domain mostly encompasses the midlatitudes which have a larger fraction of the land surface; the TRACE-P CO_2 results are for the month of March, whereas the model-derived estimates are presented as an average calculated from an annual mean. We further note that prior flux estimates do not include human or animal respiration, which for the world's most populous region is a CO_2 source that merits future consideration. Further quantification of spatial sources is feasible via use of an atmospheric transport model and inverse modeling based on CO_2 observations from continental or marine surface sites located in close proximity to the Pacific Rim coupled with the aircraft data.

7. Summary

[36] High-precision, high-resolution CO_2 data obtained during late winter/early spring point to the importance of continental CO_2 inputs to the western Pacific basin. Results emphasize that the Asian continent was a primary source of

atmospheric CO_2 and that frontal systems were an important mechanism by which emissions were propagated away from this region. The regional distribution of CO_2 was dominated by the presence of significantly higher concentrations in the extratropics west of 160°E that exhibited a decreasing trend with height, were highly correlated with latitude showing a distinct north to south gradient, and peaked between 35 and 40°N within the planetary boundary layer. Near the Asian continent, discrete plumes encountered below 2 km contained up to 393.6 ppmv CO_2 and were augmented with the combustion and industrial tracers CO, C_2H_6, C_2H_4, C_2H_2, C_3H_8, CH_3Cl, and C_2Cl_4. Coupling of the in situ data with 5-day backward trajectories and an emissions database for Asia indicated northeast Asia as the source region of these pollution events registered in the PBL. A chemically based air mass classification scheme using the combustion products CO and C_2H_2 as tracers of continental source emissions showed an excellent positive correlation for CO_2 ($r^2 = 0.98$) with respect to this ratio in the lower free troposphere. South of the Tropic of Cancer, mean and median CO_2 values derived from samples obtained below 8 km were less than those calculated for the extratropics; however within the UT of both regions, similar values were determined. The relationship between CO_2 and the C_2H_2/CO ratio suggests recent inputs from the surface to the tropical UT from both combustion and industrial sources. From these data we estimated a net export flux on the order of 14 Tg C day^{-1}, attributable to both anthropogenic emissions and the respiration of the terrestrial biosphere, animals, and humans. The TRACE-P database provides a baseline for future assessments of the impact of Asian emissions and is also available for validating the simulated results of CO_2 variations by atmospheric transport models.

[37] **Acknowledgments.** We are most grateful for the valuable contributions from Charlie Hudgins, Jim Plant, Sandy Branham, Donald Bagwell, John Barrick, and Ali Aknan during TRACE-P. It is with much appreciation that we acknowledge Tom Conway who provided the NOAA/CMDL data and helpful comments on the manuscript. We thank both the NASA Dryden DC-8 and WFF P-3B ground and flight crews for their excellent support. This research was supported by the NASA Global Tropospheric Chemistry Program.

References

Akimoto, H., and H. Narita, Distribution of SO_2, NO_x, and CO_2 emissions from fuel combustion and industrial activities in Asia with 1° × 1° resolution, *Atmos. Environ.*, *28*(2), 213–225, 1994.

Anderson, B. E., G. L. Gregory, J. E. Collins Jr., G. W. Sachse, T. J. Conway, and G. P. Whiting, Airborne observations of spatial and temporal variability of tropospheric carbon dioxide, *J. Geophys. Res.*, *101*(D1), 1985–1997, 1996.

Andres, R. J., D. J. Fielding, G. Marland, T. A. Boden, N. Kumar, and A. T. Kearney, Carbon dioxide emissions from fossil-fuel use, 1751–1950, *Tellus*, *51B*, 759–765, 1999.

Austin, J. R., and R. P. Midgley, The climatology of the jet stream and stratospheric intrusions of ozone over Japan, *Atmos. Environ.*, *28*, 39–52, 1994.

Blake, D. R., T.-Y. Chen, T. W. Smith Jr., C. J.-L. Wang, O. W. Wingenter, N. J. Blake, and F. S. Rowland, Three-dimensional distribution of nonmethane hydrocarbons and halocarbons over the northwestern Pacific during the 1991 Pacific Exploratory Mission (PEM-West A), *J. Geophys. Res.*, *101*(D1), 1763–1778, 1996.

Blake, N. J., D. R. Blake, T.-Y. Chen, J. E. Collins Jr., G. W. Sachse, B. E. Anderson, and F. S. Rowland, Distribution and seasonality of selected hydrocarbons and halocarbons over the western Pacific basin during PEM-West A and PEM-West B, *J. Geophys. Res.*, *102*(D23), 28,315–28,331, 1997.

Chen, S., Y. Kuo, P. Zhang, and Q. Bai, Synoptic climatology of cyclogenesis over East Asia, 1958–1987, *Mon. Weather Rev.*, *119*, 1407–1418, 1991.

Ciais, P., P. Peylin, and P. Bousquet, Regional biospheric carbon fluxes as inferred from atmospheric CO_2 measurements, *Ecol. Appl.*, *10*(6), 1574–1589, 2000.

Conway, T. J., P. Tans, L. S. Waterman, K. W. Thoning, K. A. Masarie, and R. H. Gammon, Atmospheric carbon dioxide measurements in the remote global troposphere, 1981–1984, *Tellus*, *40B*, 81–115, 1988.

Conway, T. J., P. P. Tans, L. S. Waterman, K. W. Thoning, D. R. Kitzis, K. A. Masarie, and N. Zhang, Evidence for interannual variability of the carbon cycle from the National Oceanic and Atmospheric Administration/Climate Monitoring and Diagnostics Laboratory Global Air Sampling Network, *J. Geophys. Res.*, *99*(D11), 22,831–22,855, 1994.

Falkowski, P., et al., The global carbon cycle: A test of our knowledge of Earth as a system, *Science*, *290*, 291–296, 2000.

Fuelberg, H. E., C. M. Kiley, J. R. Hannan, D. J. Westberg, M. A. Avery, and R. E. Newell, Atmospheric transport during the Transport and Chemical Evolution over the Pacific (TRACE-P) experiment, *J. Geophys. Res.*, *108*(D20), 8782, doi:10.1029/2002JD003092, in press, 2003.

Fung, I. Y., C. J. Tucker, and K. C. Prentice, Application of advanced very high resolution radiometer vegetation index to study atmosphere-biosphere exchange of CO_2, *J. Geophys. Res.*, *92*, 2999–3015, 1987.

Hunt, R. E., S. C. Piper, R. Nemani, C. D. Keeling, R. D. Otto, and S. W. Running, Global net carbon exchange and intra-annual atmospheric CO_2 concentrations predicted by an ecosystem process model and three-dimensional atmospheric transport model, *Global Biogeochem. Cycles*, *10*(3), 431–456, 1996.

Ing, G. K. T., A duststorm over central China, April 1969, *Weather*, *27*, 136–145, 1972.

Jacob, D. J., et al., The Transport and Chemical Evolution over the Pacific (TRACE-P) Mission: Design, execution, and first results, *J. Geophys. Res.*, *108*(D20), 8781, doi:10.1029/2002JD003276, in press, 2003.

Komhyr, W. D., L. S. Waterman, and W. R. Taylor, Semiautomatic nondispersive infrared analyzer apparatus for CO_2 air sample analyses, *J. Geophys. Res.*, *88*, 1315–1322, 1983.

Kotamarthi, V. R., and G. R. Carmichael, The long range transport of pollutants in the Pacific Rim region, *Atmos. Environ.*, *24A*(6), 1521–1534, 1990.

Liu, H., W. L. Chang, S. J. Oltmans, L. Y. Chan, and J. M. Harris, On springtime high ozone events in the lower troposphere from Southeast Asian biomass burning, *Atmos. Environ.*, *33*, 2403–2410, 1999.

Liu, H., D. J. Jacob, I. Bey, R. M. Yantosca, B. N. Duncan, and G. W. Sachse, Transport pathways for Asian combustion outflow over the Pacific: Interannual and seasonal variations, *J. Geophys. Res.*, *108*(D20), 8786, doi:10.1029/2002JD003102, in press, 2003.

Matsueda, H., and H. Y. Inoue, Measurements of atmospheric CO_2 and CH_4 using a commercial airliner from 1993 to 1994, *Atmos. Environ.*, *30*(10/11), 1647–1655, 1996.

Matsueda, H., and H. Y. Inoue, Aircraft measurements of trace gases between Japan and Singapore in October of 1993, 1996, and 1997, *Geophys. Res. Lett.*, *26*(16), 2413–2416, 1999.

Matsueda, H., H. Y. Inoue, and M. Ishii, Aircraft observation of carbon dioxide at 8–13 km altitude over the western Pacific from 1993 to 1999, *Tellus*, *54B*, 1–21, 2002.

McKeen, S. A., and S. C. Liu, Hydrocarbon ratios and photochemical history of air masses, *Geophys. Res. Lett.*, *20*, 2363–2366, 1993.

McKeen, S. A., S. C. Liu, E.-Y. Hsie, X. Lin, J. D. Bradshaw, S. Smyth, G. L. Gregory, and D. R. Blake, Hydrocarbon ratios during PEM-West A: A model perspective, *J. Geophys. Res.*, *101*, 2087–2109, 1996.

Merrill, J. T., R. Bleck, and L. Avila, Modeling atmospheric transport to the Marshall Islands, *J. Geophys. Res.*, *90*, 12,927–12,936, 1985.

Merrill, J. T., M. Uematsu, and R. Bleck, Meteorological Analysis of long-range transport of mineral aerosols over the North Pacific, *J. Geophys. Res.*, *94*(D6), 8584–8598, 1989.

Nakazawa, T., K. Miyashita, S. Aoki, and M. Tanaka, Temporal and spatial variations of upper tropospheric and lower stratospheric carbon dioxide, *Tellus*, *43B*, 106–117, 1991.

Nakazawa, T., S. Murayama, K. Miyashita, S. Aoki, and M. Tanaka, Longitudinally different variations of lower tropospheric carbon dioxide concentrations over the North Pacific Ocean, *Tellus*, *44B*, 161–172, 1992.

Nakazawa, T., S. Morimoto, S. Aoki, and M. Tanaka, Time and space variations of the carbon isotope ratio of tropospheric carbon dioxide over Japan, *Tellus*, *45B*, 258–274, 1993.

Nakicenovic, N., and R. Swart, *Emissions Scenarios, A Special Report of the Working Group III of the Intergovernmental Panel on Climate Change*, Cambridge Univ. Press, Cambridge, New York, 2000.

Pochanart, P., J. Hirokawa, Y. Kajii, and H. Akimoto, Influence of regional-scale anthropogenic activity in northeast Asia on seasonal variations of surface ozone and carbon monoxide observed at Oki, Japan, *J. Geophys. Res.*, *104*(D3), 3621–3631, 1999.

Sachse, G. W., R. C. Harriss, J. Fishman, G. F. Hill, and D. R. Cahoon, Carbon monoxide over the Amazon basin during the 1985 dry season, *J. Geophys. Res.*, *93*, 1422–1430, 1988.

Siddiqi, T. A., Carbon dioxide emissions from the use of fossil fuels in Asia: An overview, *Ambio*, *25*(4), 229–232, 1996.

Singh, H. B., and P. B. Zimmerman, Atmospheric distribution and sources of nonmethane hydrocarbons, in *Gaseous Pollutants: Characterization and Cycling*, edited by J. O. Nriagu, pp. 177–235, John Wiley, Hoboken, N. J., 1992.

Smyth, S., et al., Comparison of free tropospheric western Pacific air mass classification schemes for PEM-West A experiment, *J. Geophys. Res.*, *101*(D1), 1743–1762, 1996.

Smyth, S., et al., Characterization of the chemical signatures of air masses observed during the PEM experiments over the western Pacific, *J. Geophys. Res.*, *104*(D13), 16,243–16,254, 1999.

Streets, D. G., et al., An inventory of gaseous and primary aerosol emissions in Asia in the year 2000, *J. Geophys. Res.*, *108*(D21), 8809, doi:10.1029/2002JD003093, in press, 2003.

Talbot, R. W., et al., Large-scale distributions of tropospheric nitric, formic, and acetic acids over the western Pacific basin during wintertime, *J. Geophys. Res.*, *102*(D23), 28,303–28,313, 1997.

Tanaka, M., T. Nakazawa, and S. Aoki, Concentration of atmospheric carbon dioxide over Japan, *J. Geophys. Res.*, *88*(C2), 1339–1344, 1983.

Tanaka, M., T. Nakazawa, and S. Aoki, Time and space variations of tropospheric carbon dioxide over Japan, *Tellus*, *39B*, 3–12, 1987.

Tanaka, M., T. Nakazawa, S. Aoki, and H. Ohshima, Aircraft measurements of tropospheric carbon dioxide over the Japanese islands, *Tellus*, *40B*, 16–22, 1988.

Thornhill, K. L., B. E. Anderson, J. D. W. Barrick, D. R. Bagwell, R. Friesen, and D. H. Lenschow, Air motion intercomparison flights during TRACE-P/ACE-ASIA, *J. Geophys. Res.*, *108*(D20), 8783, doi:10.1029/2002JD003180, in press, 2003.

Vay, S. A., B. E. Anderson, T. J. Conway, G. W. Sachse, J. E. Collins Jr., D. R. Blake, and D. J. Westberg, Airborne observations of the tropospheric CO_2 distribution and its controlling factors over the South Pacific basin, *J. Geophys. Res.*, *104*(D5), 5663–5676, 1999.

Watanabe, F., O. Uchino, Y. Joo, M. Aono, K. Higashijima, Y. Hirano, K. Tsuboi, and K. Suda, Interannual variation of growth rate of atmospheric carbon dioxide concentration observed at the JMA's three monitoring stations: Large increase in concentration of atmospheric carbon dioxide in 1998, *J. Meteorol. Soc. Jpn.*, *78*(5), 673–682, 2000.

Woo, J. H., et al., The contribution of biomass and biofuel emissions to trace gas distributions in Asia during the TRACE-P experiment, *J. Geophys. Res.*, *108*(D21), 8812, doi:10.1029/2002JD003200, in press, 2003.

Yienger, J. J., M. Galanter, T. A. Holloway, M. J. Phadnis, S. K. Guttikunda, G. R. Carmichael, W. J. Moxim, and H. Levy II, The episodic nature of air pollution transport from Asia to North America, *J. Geophys. Res.*, *105*(D22), 26,931–26,945, 2000.

B. Anderson, M. Avery, and S. Vay, NASA Langley Research Center, MS 483, Hampton, VA 23681-2199, USA. (b.e.anderson@larc.nasa.gov; m.a.avery@larc.nasa.gov; s.a.vay@larc.nasa.gov)

D. R. Blake, Department of Chemistry, University of California, Irvine, 570 Rowland Hall, Irvine, CA 92697-2025, USA. (dblake@orion.oac.uci.edu)

C. Kiley, Department of Meteorology, Florida State University, Love Building, Room 309, Mail Code 4520, Tallahassee, FL 32306-4520, USA. (ckiley@met.fsu.edu)

S. Nolf, Computer Sciences Corporation, 21 Enterprise Parkway, 262-3501, Hampton, VA 23666, USA. (snolf@csc.com)

G. Sachse, NASA Langley Research Center, MS 472, Hampton, VA 23681-2199, USA. (g.w.sachse@larc.nasa.gov)

D. G. Streets, Decision and Information Sciences Division, Argonne National Laboratory, DIS/900, 9700 South Cass Avenue, Argonne, IL 60439, USA. (dstreets@anl.gov)

L. Thornhill and D. Westberg, SAIC, 22 Enterprise Parkway, Suite 200, Hampton, VA 23666, USA. (k.l.thornhill@larc.nasa.gov; d.j.westberg@larc.nasa.gov)

Y. Tsutsumi, Atmospheric Environmental Division, Japan Meteorological Agency, 1-3-4 Otemachi Chiyoda-Ky, Tokyo 100-8122, Japan. (y-tsutsumi@met.kishou.go.jp)

J.-H. Woo, Center for Global and Regional Environmental Research, University of Iowa, Iowa City, IA 52242, USA. (woojh21@cgrer.uiowa.edu)